



ELSEVIER

Nuclear Physics A 690 (2001) 790–800



www.elsevier.nl/locate/npe

Electron screening effect in the reactions ${}^3\text{He}(d, p){}^4\text{He}$ and $d({}^3\text{He}, p){}^4\text{He}$ [☆]

M. Aliotta ^{a,1}, F. Raiola ^a, G. Gyürky ^b, A. Formicola ^a, R. Bonetti ^c,
C. Brogginì ^d, L. Campajola ^e, P. Corvisiero ^f, H. Costantini ^f,
A. D'Onofrio ^g, Z. Fülöp ^b, G. Gervino ^h, L. Gialanella ^e, A. Guglielmetti ^c,
C. Gustavino ⁱ, G. Imbriani ^{e,j}, M. Junker ⁱ, P.G. Moroni ^f, A. Ordine ^e,
P. Prati ^f, V. Roca ^e, D. Rogalla ^a, C. Rolfs ^a, M. Romano ^e, F. Schümann ^a,
E. Somorjai ^b, O. Straniero ^k, F. Strieder ^a, F. Terrasi ^g, H.P. Trautvetter ^a,
S. Zavatarelli ^f

^a Institut für Physik mit Ionenstrahlen, Ruhr-Universität Bochum, Bochum, Germany

^b Atomki, Debrecen, Hungary

^c Dipartimento di Fisica, Università di Milano and INFN, Milano, Italy

^d INFN, Padova, Italy

^e Dipartimento di Scienze Fisiche, Università Federico II and INFN, Napoli, Italy

^f Dipartimento di Fisica, Università di Genova and INFN, Genova, Italy

^g Dipartimento di Scienze Ambientali, Seconda Università di Napoli, Caserta and Napoli, Italy

^h Dipartimento di Fisica Sperimentale, Università di Torino and INFN, Torino, Italy

ⁱ Laboratori Nazionali del Gran Sasso dell'INFN, Assergi, Italy

^j Osservatorio Astronomico di Capodimonte, Napoli, Italy

^k Osservatorio Astronomico di Collurania, Teramo, Italy

Received 27 November 2000; revised 9 January 2001; accepted 10 January 2001

Abstract

The cross section of the reactions ${}^3\text{He}(d, p){}^4\text{He}$ and $d({}^3\text{He}, p){}^4\text{He}$ has been measured at the center-of-mass energies $E = 5$ to 60 keV and 10 to 40 keV, respectively. The experiments were performed to determine the magnitude of the electron screening effect leading to the respective electron-screening potential energy $U_e = 219 \pm 7$ and 109 ± 9 eV, which are both significantly higher than the respective values from atomic physics models, $U_e = 120$ and 65 eV. © 2001 Elsevier Science B.V. All rights reserved.

[☆] Supported in part by INFN, BMBF (06BO812), DFG (436UNG113-146) and OTKA (T025465).

E-mail address: rolfs@ep3.ruhr-uni-bochum.de (C. Rolfs).

¹ Alexander von Humboldt Fellow.

1. Introduction

Due to the Coulomb barrier of the entrance channel, the cross section $\sigma(E)$ of a fusion reaction drops exponentially with decreasing center-of-mass energy E ,

$$\sigma(E) = S(E)E^{-1} \exp(-2\pi\eta), \quad (1)$$

where η is the Sommerfeld parameter and $S(E)$ is the astrophysical S-factor [1,2]. The parametrisation assumes that the Coulomb barrier is that resulting from bare nuclei. However, for nuclear reactions studied in the laboratory, the target nuclei and the projectiles are usually in the form of neutral atoms or molecules and ions, respectively. The resulting enhancement of the electron-screened cross section, $\sigma_s(E)$, over that for bare nuclei, $\sigma_b(E)$, is described by the expression [3–5]

$$\sigma_s(E)/\sigma_b(E) = (S_s(E)/S_b(E))(E/E + U_e) \exp(\pi\eta U_e/E), \quad (2)$$

where U_e is the constant electron-screening potential energy, and $S_s(E)$ and $S_b(E)$ is the S-factor for screened and bare nuclides, respectively.

The exponential enhancement has been observed in several fusion reactions [6–14], at energies from a few keV to a few tens of keV. However, the observed enhancements were significantly larger than could be accounted for from the adiabatic limit, i.e., the difference in electron binding energies between the colliding atoms and the compound atom. The most pronounced excess has been reported for the ${}^3\text{He}(d, p){}^4\text{He}$ reaction ($Q = 18.4$ MeV), $U_e = 186 \pm 9$ eV [9], significantly larger than the adiabatic limit $U_e = 120$ eV. In the analysis of such data, the effective energy in the target has to be known precisely and always involves energy-loss corrections. In [6,9], the authors used energy-loss values for deuterons in helium as tabulated [15], which were derived by extrapolation of data for deuterons above 80 keV to lower energies. However, energy-loss measurements of low-energy protons and deuterons in helium gas found [16] significantly lower values than tabulated [15]. Using these lower values, a reanalysis of the ${}^3\text{He}(d, p){}^4\text{He}$ data led [17] to $U_e = 134 \pm 8$ eV. Recent measurements of the stopping power of low-energy deuterons in ${}^3\text{He}$ gas observed [18,19] a threshold effect near $E_d = 18$ keV (Fig. 1). The data disagree significantly with the results reported in [16] (Fig. 1) and cast doubt on the reliability of the ${}^3\text{He}(d, p){}^4\text{He}$ data analyses [6,9,17].

For the inverted reaction, $d({}^3\text{He}, p){}^4\text{He}$, a value of $U_e = 123 \pm 9$ eV has been reported [9], while the united-atom model (including a Coulomb-explosion process of the D_2 target molecules) led to the estimate $U_e = 65$ eV [6] (see however [20]). Recently, the cross section of this reaction was restudied at the LUNA facility for $E = 4$ to 14 keV including a measurement of the associated stopping power [14]. The observed stopping power values were in good agreement with the standard compilation [15]. The data together with results from previous work at higher energies led to $U_e = 132 \pm 9$ eV, where renormalisations in the absolute scale of the various data sets had to be carried out. In order to improve the data set, a renewed measurement of this reaction at higher energies using the same LUNA setup appeared desirable.

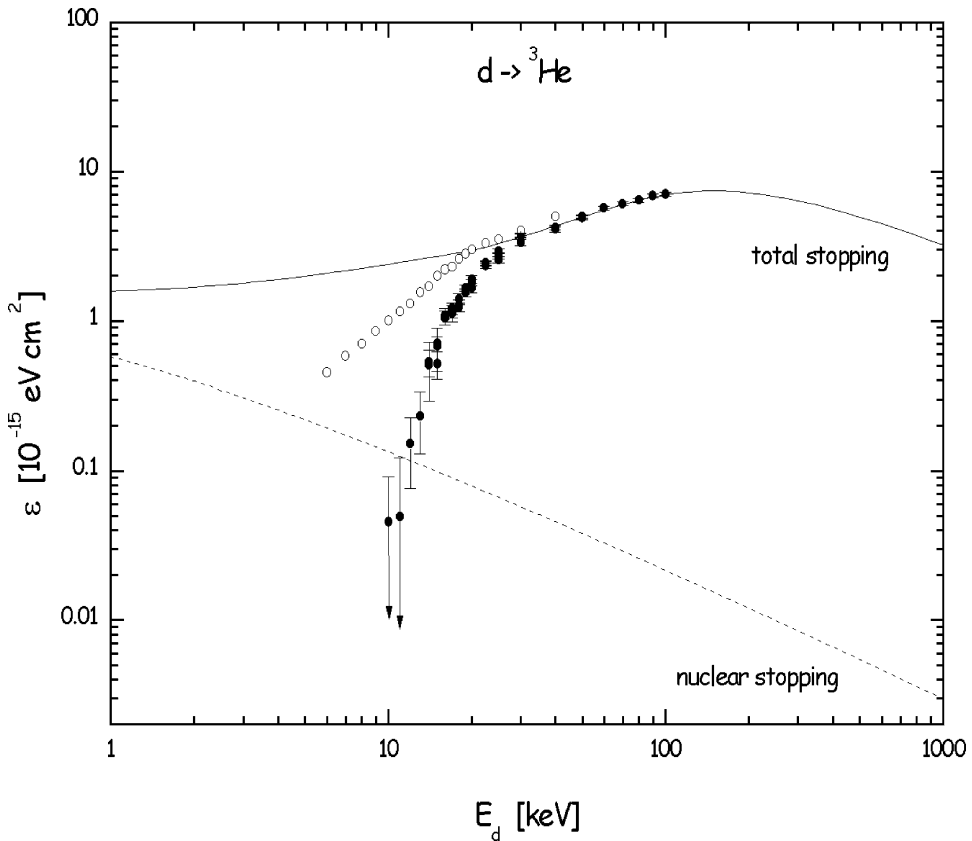


Fig. 1. Stopping power ε of deuterons in ${}^3\text{He}$ gas as function of deuteron energy. The total stopping power curve is obtained from the compilation [15] based on data above 80 keV. The nuclear stopping power curve is the prediction from [15]. The filled-circle data points [18,19] show a threshold effect near $E_d = 18$ keV. Also shown are the previous results using time-of-flight spectroscopy [16] (open-circle data points) exhibiting no threshold effect.

As part of an ongoing program on electron-screening effects, we have restudied with the LUNA setup the cross section of ${}^3\text{He}(d,p){}^4\text{He}$ at $E = 5$ to 60 keV and $d({}^3\text{He},p){}^4\text{He}$ at $E = 10$ to 40 keV.

2. Setup

The measurements were carried out at the 100 kV accelerator of the Ruhr-Universität Bochum [21] involving the LUNA setup [12,13,22,23]. Briefly, the absolute incident ion beam energy, E_{lab} , was known to a precision of 5×10^{-5} , and the beam energy spread was found to be 0.10 keV at $E_{\text{lab}} = 20$ keV. The beam entered (Fig. 2) the target chamber of a differentially pumped gas-target system through 3 apertures (A_1 , A_2 , and A_3) of high gas-flow impedance (respective diameters = 15, 10, and 7 mm; respective lengths

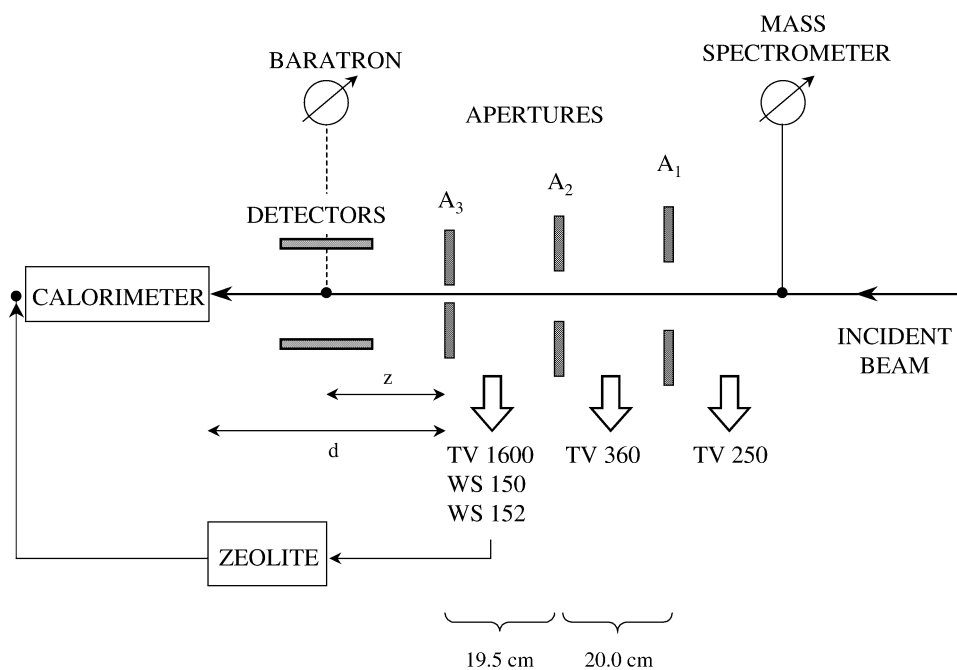


Fig. 2. Schematic diagram of the experimental setup. The ion beam enters the target chamber through the apertures A_1 , A_2 and A_3 of high pumping impedance and is stopped in a calorimeter. The differentially pumping stages consist of turbo pumps (e.g., TV1600 = 1600 l/s pumping speed) and Roots blowers (e.g., WS150 = 150 m³/h pumping speed). The ³He gas from the 3 pumping stages is passed through a zeolite trap cooled to liquid nitrogen temperature and fed back into the target chamber. The gas pressure at the location of the detectors is measured with a Baratron capacitance manometer. The gas composition is monitored using a mass spectrometer.

= 80, 80, and 60 mm) and was stopped in a calorimeter (4 W power) with an active area of 3.5 cm diameter. The ³He gas pressure in the target chamber ($P = 0.0050$ to 0.250 mbar) and the D₂ gas pressure ($P = 0.0050$ mbar) were measured with a Baratron capacitance manometer to a relative accuracy of better than 1% and a systematic accuracy of 1%. The ³He target gas was recirculated and cleaned using a zeolite trap; the resulting gas composition was monitored with a mass spectrometer: no contaminants were observed ($\leq 0.1\%$). The D₂ target gas was not recirculated. Beam-heating effects on the gas density have been included by an additional 1% accidental error. For $P(^3\text{He}) = 0.25$ mbar, the system reduced the pressure to 2×10^{-4} , 1×10^{-5} , and 1×10^{-6} mbar in the regions between the apertures A_3 and A_2 , A_2 and A_1 , and beyond A_1 , respectively. A similar reduction was observed at other ³He or D₂ pressure values. The main pressure drop occurred across the entrance aperture A_3 , while the extended target zone between A_3 and the calorimeter (length $d = 43.0 \pm 0.1$ cm) was characterized by a constant gas pressure. For each run, the average power deposited by the beam on the calorimeter was deduced from the difference between transistor powers needed to keep the beam dump at the same temperature, with the beam off and on. The statistical error on the measured power

difference was obtained by adding in quadratures the errors on the measured powers (1% relative error each), while a systematical error of 2% on the beam power was also taken into account. Finally, the beam power was converted into beam current using the beam energy at the calorimeter, i.e., the incident energy minus the energy loss in the whole target gas; the uncertainty in the latter quantity was — for all incident energies — negligible with respect to the accuracy of the beam power.

The detector setup consisted of eight, 1 mm thick Si detectors of $5 \times 5 \text{ cm}^2$ area (each) placed around the beam axis: they formed a 14 cm long parallelepiped in the target chamber. Each detector was shielded by a $25 \mu\text{m}$ thick Ni foil in order to stop the ^4He ejectiles, the elastic scattering products, and the light induced by the beam. A NE102A plastic scintillator ($1 \times 1 \text{ m}^2$ area, 3.5 cm thickness; not shown in Fig. 2) was placed below the target chamber and used to veto cosmic-ray-induced events in the detectors. Dead time effects in the detectors were monitored using a pulser and were kept below 3%. A sample spectrum for one of the Si detectors is illustrated in Fig. 3. The detection efficiency in the setup, $\eta = 0.201 \pm 0.004$, was calculated with a Monte Carlo simulation [14,23].

In going through the gas of the target chamber, the beam experienced a mean energy loss ΔE to the middle of the detector setup (at a distance $z = 18.5 \pm 0.1 \text{ cm}$ from the middle

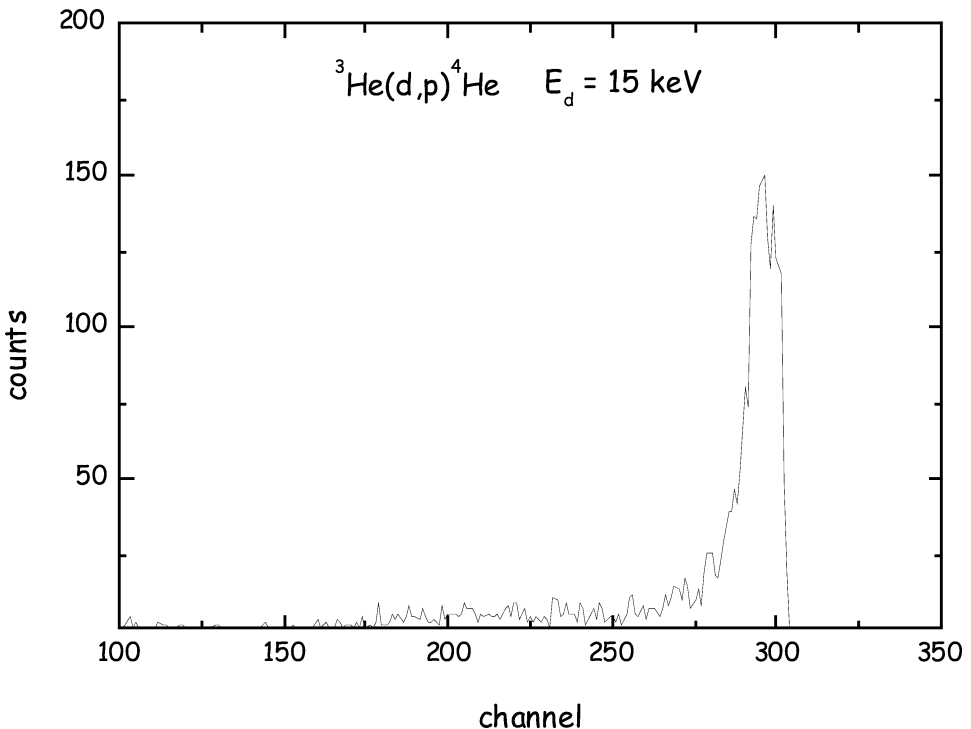


Fig. 3. Spectrum for the $^3\text{He}(d,p)^4\text{He}$ reaction ($Q = 18.4 \text{ MeV}$) obtained at $E_d = 15 \text{ keV}$. The peak corresponds to the 14.7 MeV protons fully stopped in the Si detector, while the low-energy tail represents protons losing only a fraction of their energy in the detector. The reaction yield was deduced from the number of counts in both the peak and tail.

of the entrance aperture A_3). This was taken into account by introducing an effective energy $E_{\text{eff}} = E$ corresponding to the mean value of the beam energy distribution in the detector setup, evaluated by Monte Carlo simulations. Values for ΔE were derived from Fig. 1 [18,19].

3. Procedures and results

At a given incident beam energy, the cross section $\sigma(E)$ is related to the number of observed protons, N , from the reaction ${}^3\text{He}(d,p){}^4\text{He}$ or $d({}^3\text{He},p){}^4\text{He}$ (in the detector setup) by the equation

$$N = N_p N_t \eta d \sigma(E), \quad (3)$$

where N_p is the number of incident projectiles (deduced from the calorimeter), N_t is the number of target atoms per unit of volume (deduced from the gas pressure), and E is the effective energy within the target (in the center-of-mass system).

Most measurements were carried out at a pressure $P = 0.0050$ mbar corresponding to a few monolayers of target material (e.g., 6×10^{15} ${}^3\text{He}$ atoms/cm² for $d = 43$ cm). In turn, the energy loss in the gas can be neglected: at the lowest atomic deuteron energy of $E_d = 13$ keV and for ${}^3\text{He}$ gas ($E = 7.8$ keV), one finds $\Delta E_{\text{lab}} = 1.4$ eV (Fig. 1). The exceptions are the measurements of ${}^3\text{He}(d,p){}^4\text{He}$ at ultra-low energies, where a ${}^3\text{He}$ pressure $P = 0.250$ mbar was used: at the lowest energy $E_d = 8.35$ keV ($E = 5.01$ keV) one finds $\Delta E_{\text{lab}} \approx 28$ eV for $d = 43$ cm and 12 eV for $z = 18.5$ cm leading to an error in cross section of about 2%, which we have neglected.

As just discussed, an atomic deuteron beam (D_1^+) was used for the ${}^3\text{He}(d,p){}^4\text{He}$ studies at higher energies, while a diatomic (D_2^+) or triatomic (D_3^+) beam was employed at ultra-low energies. Since the molecular beam breaks up quickly in the ${}^3\text{He}$ target gas [24–28], one arrives at the equivalent deuteron beam energy $E_d = E_{d2}/2$ or $E_{d3}/3$ with a nearly twofold or threefold increase in current. The energy spread ΔE_d of the resulting deuteron beam due to the effects of Coulomb explosion of the molecular beam is estimated to be at most $\Delta E_d = 0.5$ keV at $E_d = 10$ keV. Since the Coulomb explosion has been found to be “gentle” [24–28], the actual spread ΔE_d is significantly smaller. The good agreement of the data points obtained with the atomic and diatomic beams at nearly overlapping energies confirms that the effects of Coulomb explosion are negligible for the observed features.

The results for the ${}^3\text{He}(d,p){}^4\text{He}$ and $d({}^3\text{He},p){}^4\text{He}$ reactions — in form of the astrophysical $S(E)$ factor — are summarized in Tables 1 and 2 and displayed in Figs. 4 and 5, respectively. The absolute $S(E)$ values for both reactions are in fair agreement with previous work [6,9,14,21,29] within the quoted uncertainties.

4. Discussion

For the analysis of electron screening effects, one must extrapolate the bare cross section $\sigma_b(E)$ at high energies ($E > 40$ keV) to low energies. This extrapolation appears to be

Table 1
Excitation function of ${}^3\text{He}(\text{d}, \text{p}){}^4\text{He}$

E^{a} (keV)	$P({}^3\text{He})^{\text{b}}$ (mbar)	$S(E)^{\text{c}}$ (MeV b)
		Atomic deuterons (D_1^+)
7.80	0.0050	8.66 ± 0.28
8.96	0.0050	7.85 ± 0.26
9.66	0.1000	7.68 ± 0.22
10.72	0.0050	7.48 ± 0.20
11.44	0.0050	7.29 ± 0.20
11.99	0.0050	7.35 ± 0.20
13.18	0.0050	7.28 ± 0.20
14.39	0.0050	7.04 ± 0.20
14.99	0.0050	7.07 ± 0.20
16.75	0.0050	7.16 ± 0.20
17.99	0.0050	7.02 ± 0.20
19.14	0.0050	7.20 ± 0.20
20.94	0.0050	6.81 ± 0.18
21.55	0.0050	7.09 ± 0.20
22.71	0.0050	7.13 ± 0.20
23.93	0.0050	6.91 ± 0.18
25.08	0.0050	7.18 ± 0.20
26.62	0.0050	6.93 ± 0.18
28.73	0.0050	7.22 ± 0.20
29.91	0.0050	6.87 ± 0.18
31.10	0.0050	7.24 ± 0.20
32.89	0.0050	7.04 ± 0.20
33.49	0.0050	7.33 ± 0.20
35.86	0.0050	7.22 ± 0.18
38.58	0.0050	7.33 ± 0.18
40.67	0.0050	7.44 ± 0.22
41.87	0.0050	7.29 ± 0.20
43.06	0.0050	7.48 ± 0.22
44.85	0.0050	7.40 ± 0.20
45.44	0.0050	7.70 ± 0.22
47.86	0.0050	7.63 ± 0.20
50.21	0.0050	7.66 ± 0.22
50.83	0.0050	7.70 ± 0.20
52.65	0.0050	7.70 ± 0.22
53.82	0.0050	7.77 ± 0.22
55.04	0.0050	7.77 ± 0.22
56.81	0.0050	7.88 ± 0.20
57.41	0.0050	7.94 ± 0.22
59.80	0.0050	8.12 ± 0.22

(continued)

Table 1 — continued

E^a (keV)	$P(^3\text{He})^b$ (mbar)	$S(E)^c$ (MeV b)
Diatomic deuterons (D_2^+)		
6.02	0.2500 ^d	10.37 ± 0.35
6.45	0.2500 ^d	9.36 ± 0.35
6.90	0.2500 ^d	8.82 ± 0.31
7.51	0.2500 ^d	9.12 ± 0.29
8.18	0.2500 ^d	8.31 ± 0.24
9.02	0.1000 ^d	7.88 ± 0.22
Triatomic deuterons (D_3^+)		
5.01	0.2500 ^d	10.76 ± 1.47
5.50	0.2500 ^d	10.31 ± 0.81
6.01	0.2500 ^d	9.41 ± 0.48

^a Equivalent atomic deuteron energy in case of molecular deuterons (all in the center-of-mass system).

^b Gas pressure in the target chamber.

^c Errors quoted include only statistical and accidental (2.6%) uncertainties; a systematical error of 3% (1% pressure, 2% calorimeter, 2% efficiency) for the absolute values has to be added to the quoted errors.

^d The energy loss of deuterons in ^3He gas at these pressures was obtained from the data shown in Fig. 1 [18,19].

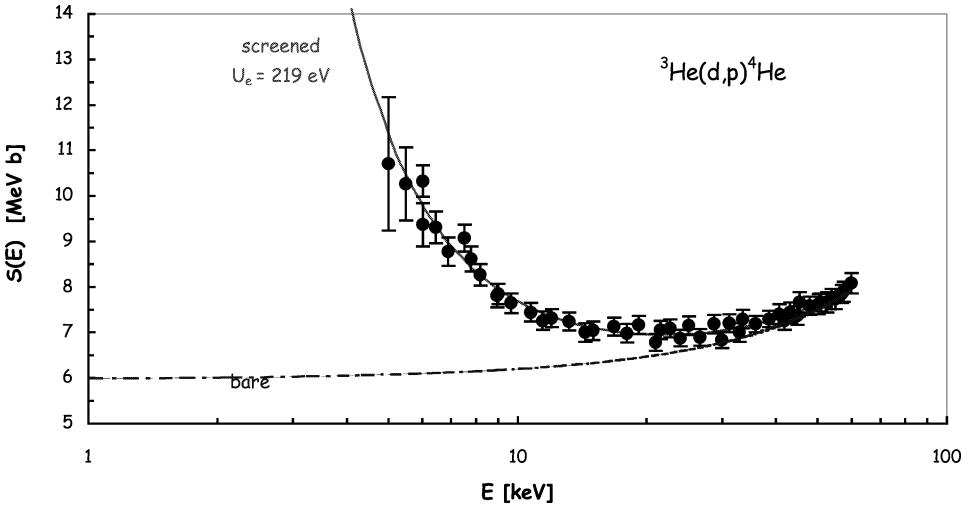


Fig. 4. $S(E)$ factor data for the $^3\text{He}(d,p)^4\text{He}$ reaction from the present work. The errors shown represent only statistical and accidental uncertainties, which were used in the fits. The dashed curve represents the $S(E)$ factor for bare nuclei and the solid curve that for screened nuclei with $U_e = 219$ eV.

Table 2
Excitation function of $d(^3\text{He}, p)^4\text{He}$

E^a (keV)	$P(\text{D}_2)^b$ (mbar)	$S(E)^c$ (MeV b)
11.95	0.0050	7.19 ± 0.35
13.95	0.0050	6.95 ± 0.23
15.95	0.0050	6.87 ± 0.18
17.94	0.0050	6.91 ± 0.19
19.93	0.0050	6.75 ± 0.18
21.92	0.0050	6.96 ± 0.19
23.92	0.0050	6.92 ± 0.19
25.92	0.0050	7.17 ± 0.19
27.88	0.0050	7.01 ± 0.19
29.88	0.0050	7.19 ± 0.19
31.90	0.0050	7.17 ± 0.19
33.89	0.0050	7.43 ± 0.20
35.89	0.0050	7.39 ± 0.19
35.89	0.0050	7.58 ± 0.20
37.88	0.0050	7.63 ± 0.20
39.87	0.0050	7.65 ± 0.20

^a Center-of-mass energy within the target.

^b Gas pressure in the target chamber.

^c Errors quoted include only statistical and accidental (2.6%) uncertainties; a systematical error of 3% (1% pressure, 2% calorimeter, 2% efficiency) for the absolute values has to be added to the quoted errors.

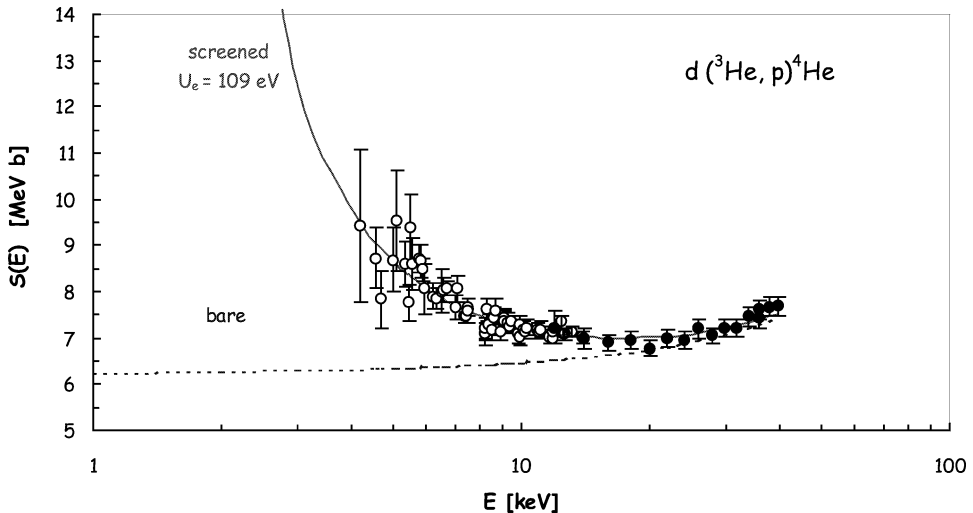


Fig. 5. $S(E)$ factor data for the $d(^3\text{He}, p)^4\text{He}$ reaction from previous work [14] (open points) and present work (filled-in points), both obtained with the same LUNA setup. The errors shown represent only statistical and accidental uncertainties, which were used in the fits. The dashed curve represents the $S(E)$ factor for bare nuclei and the solid curve that for screened nuclei with $U_e = 109$ eV.

sufficiently well under control. For example, the parametrisation [30] of the available data for energies $E = 40$ keV to 10 MeV predicts an $S_b(E)$ factor at low energies, which agrees well with the one calculated in a microscopic cluster model [31]. Recent measurements at $E = 36$ to 385 keV included also a polarized deuteron beam [32] and led to a consistent $S_b(E)$ energy dependence at low energies, which we have adopted: $S_b(E) = 6.70 + 2.43 \times 10^{-2}E + 2.06 \times 10^{-4}E^2$ MeV b (with E in keV).

With the $S_b(E)$ function (including a free normalisation factor F), the resulting fit of the ${}^3\text{He}(d, p){}^4\text{He}$ data (Fig. 4) led to $U_e = 219 \pm 7$ eV (one standard deviation error) with a reduced $\chi^2 = 0.41$ and $F = 0.89$. The corresponding $S(E)$ factor curves for bare and screened nuclei are shown in Fig. 4 as dashed and solid curves, respectively. The experimental U_e value is consistent with previous work [9] but much larger than the adiabatic limit. The observed U_e value is not understood at present. The difference in the U_e values between [17] and the present work arises predominantly from different stopping power values used.

Similarly, the resulting fit to the $d({}^3\text{He}, p){}^4\text{He}$ data (Fig. 5) led to $U_e = 109 \pm 9$ eV with $\chi^2 = 0.88$ and $F = 0.93$ (previous work [14] $F = 0.93$), consistent with the above result within experimental uncertainties. The corresponding $S(E)$ factor curves for bare and screened nuclei are shown in Fig. 5 as dashed and solid curves, respectively. The experimental U_e value is not inconsistent with previous work [14] but much larger than the expected value of 65 eV and not understood at present. It should be noted that theoretical estimates of the screening effect on molecular targets [20] showed a dependence on the molecular orientation and require a dynamical treatment. For the $d + d$ system a larger screening potential energy has been found for molecular targets with respect to atomic ones which is caused by the symmetry of target and projectile and is not expected to hold in the general case.

In summary, the present work provides new data for two reactions down to ultra-low energies using a new setup compared to previous work and measuring [18,19] the crucial energy loss behaviour of the projectiles in the target over the relevant energy range. In order to improve the understanding of electron screening for the two reactions, a direct measurement of $S_b(E)$ is highly desirable, which could possibly be achieved with the Trojan horse method [33]. Furthermore, additional theoretical work on the effects of electron screening could improve the present understanding.

References

- [1] W.A. Fowler, Rev. Mod. Phys. 56 (1984) 149.
- [2] C. Rolfs, W.S. Rodney, Cauldrons in the Cosmos, University of Chicago Press, 1988.
- [3] H.J. Assenbaum, K. Langanke, C. Rolfs, Z. Phys. A 327 (1987) 461.
- [4] T.D. Shoppa, S.E. Koonin, K. Langanke, R. Seki, Phys. Rev. C 48 (1993) 837.
- [5] G. Fiorentini, R.W. Kavanagh, C. Rolfs, Z. Phys. A 350 (1995) 289.
- [6] S. Engstler et al., Phys. Lett. B 202 (1988) 179.
- [7] S. Engstler et al., Z. Phys. A 342 (1992) 471.
- [8] C. Angulo et al., Z. Phys. A 345 (1993) 231.
- [9] P. Prati et al., Z. Phys. A 350 (1994) 171.

- [10] U. Greife et al., *Z. Phys. A* 351 (1995) 107.
- [11] D. Zahnow, *Z. Phys. A* 359 (1997) 211.
- [12] M. Junker et al., *Phys. Rev. C* 57 (1998) 2700.
- [13] R. Bonetti et al., *Phys. Rev. Lett.* 82 (1999) 5205.
- [14] H. Costantini et al., *Phys. Lett. B* 482 (2000) 43.
- [15] H. Andersen, J.F. Ziegler, *The Stopping and Ranges of Ions in Matter*, Pergamon, New York, 1977, and SRIM-2000.
- [16] R. Golser, D. Semrad, *Phys. Rev. Lett.* 66 (1991) 1831.
- [17] K. Langanke, T.D. Shoppa, C.A. Barnes, C. Rolfs, *Phys. Lett. B* 369 (1996) 211.
- [18] A. Formicola et al., *Eur. Phys. J. A* 8 (2000) 43.
- [19] F. Raiola et al., submitted to *Nucl. Phys.*
- [20] T.D. Shoppa et al., *Nucl. Phys. A* 605 (1996) 387.
- [21] A. Krauss et al., *Nucl. Phys. A* 465 (1987) 150.
- [22] U. Greife et al., *Nucl. Instrum. Methods A* 350 (1994) 327.
- [23] C. Arpesella et al., *Nucl. Instrum. Methods A* 360 (1995) 607.
- [24] B. Meierjohann, W. Seibt, *Z. Phys.* 225 (1969) 9.
- [25] B. Meierjohann, M. Vogler, *J. Phys. B* 9 (1976) 1801.
- [26] M. Vogler, W. Seibt, *Z. Phys.* 210 (1968) 337.
- [27] M. Vogler, B. Meierjohann, *Z. Phys. A* 283 (1977) 11.
- [28] M. Vogler, B. Meierjohann, *J. Chem. Phys.* 69 (1978) 2450.
- [29] W. Möller, F. Besenbacher, *Nucl. Instrum. Methods* 168 (1980) 111.
- [30] G.S. Chulik, Y.E. Kim, R.A. Rice, M. Rabinowitz, *Nucl. Phys. A* 551 (1993) 255.
- [31] G. Blüge, K. Langanke, *Phys. Rev. C* 41 (1990) 1191.
- [32] W.H. Geist et al., *Phys. Rev. C* 60 (1999) 54003.
- [33] M. Aliotta et al., *Eur. Phys. J.*, in press.